

Pressure Effects on the Photoreactions of the Iron Acyl Complex $(\eta^5\text{-C}_5\text{H}_5)\text{Fe}(\text{CO})_2(\text{COCH}_3)$. Mechanistic Implications Regarding Competitive Reactions of the Solvento Intermediate $(\eta^5\text{-C}_5\text{H}_5)\text{Fe}(\text{CO})(\text{Sol})(\text{COCH}_3)$

David W. Ryba, Rudi van Eldik,*† and Peter C. Ford*‡

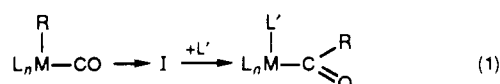
Institut für Anorganische Chemie, Universität Witten/Herdecke, Stockumer Strasse 10, 5810 Witten, Germany, and Department of Chemistry, University of California, Santa Barbara, California 93106

Received June 22, 1992

Photolysis of $\text{CpFe}(\text{CO})_2(\text{COCH}_3)$ ($\text{Cp} = \eta^5\text{-C}_5\text{H}_5$) plus $\text{P}(\text{OCH}_3)_3(\text{L})$ in *n*-heptane solutions leads to the competitive decarbonylation to give $\text{CpFe}(\text{CO})_2\text{CH}_3$ and ligand substitution to give $\text{CpFe}(\text{CO})\text{L}(\text{COCH}_3)$. The application of hydrostatic pressure changes the relative quantum yields of the two processes, higher pressure strongly favoring the ligand photosubstitution pathway. These differences are interpreted in terms of the competitive reactions of the solvento intermediate $\text{CpFe}(\text{CO})(\text{Sol})(\text{COCH}_3)$ (S), shown previously (*J. Am. Chem. Soc.* 1991, 113, 9524-9528) to be formed by the initial photolysis step, i.e., the labilization of CO. The much more negative apparent activation volume for the ligand substitution pathway suggests that this proceeds via an associative mechanism of S, while the competing methyl migration to the metal may require simultaneous dissociation of the coordinated solvent molecule, Sol.

Introduction

Recent studies in our laboratories have used photochemical techniques to prepare and to interrogate organometallic intermediates for reactions integral to proposed mechanisms for catalytic activation of CO, H₂, and other small molecules.¹ Such a reaction is the migratory insertion of CO into metal-alkyl bonds, generally considered a key step in the catalytic hydroformylation of alkenes and other industrially important carbonylations.² Previous investigators have concluded that the initial step involves alkyl migration to coordinated CO to give an intermediate which is subsequently trapped by a ligand to give the acyl product,³ for example



The reverse process, namely decarbonylation of the metal acetyl, can be effected by photolysis, presumably by ligand labilization to give the unsaturated intermediate I which undergoes subsequent methyl migration to the metal center. Recently we reported flash photolysis studies of the photochemical decarbonylation of $\text{CpFe}(\text{CO})_2(\text{COCH}_3)$ (A, $\text{Cp} = \eta^5\text{-C}_5\text{H}_5$) using time-resolved infrared (TRIR) detection techniques to probe the nature and kinetics of the reactive intermediate(s) in various solvents.⁴ Those

experiments revealed the formation of a monocarbonyl intermediate which undergoes methyl migration to give $\text{CpFe}(\text{CO})_2\text{CH}_3$ (B) in competition with trapping by ligands L to give the substituted acyl product $\text{CpFe}(\text{CO})\text{L}(\text{COCH}_3)$ (C). The solvent dependence of ν_{CO} for the terminally bound CO indicated this intermediate to be the solvento species $\text{CpFe}(\text{CO})(\text{Sol})(\text{COCH}_3)$ (S). As Scheme I illustrates, several competing pathways are available to S, although reaction with CO does not compete effectively with methyl migration in ambient temperature cyclohexane. This was evidenced by the P_{CO} (up to 1 atm) independence of the lifetime of S determined by TRIR and of Φ_{B} , the quantum yield for formation of B determined by continuous photolysis methods.⁴ In contrast, ligands such as PPh_3 and $\text{P}(\text{OCH}_3)_3$ (see below) are more reactive.

Despite the additional insight from the TRIR experiments regarding the nature of S, a likely intermediate along the thermal migratory insertion pathway as well as that leading to photodecarbonylation of A, there remain important mechanistic questions regarding how the methyl migration and ligand substitution steps of this species occur. Described here is an extension of the continuous photolysis experiments which uses hydrostatic pressure effects on the photoreaction quantum yields to provide a different perspective into the natures of those competitive steps.

Experimental Section

$\text{CpFe}(\text{CO})_2(\text{COCH}_3)$ and $\text{CpFe}(\text{CO})_2\text{CH}_3$ were prepared using published procedures.⁵ The substituted acyl complex C ($\text{L} = \text{P}(\text{OCH}_3)_3$) was prepared in situ by exhaustive photolysis of $\text{CpFe}(\text{CO})_2(\text{COCH}_3)$ under limiting concentrations of $\text{P}(\text{OCH}_3)_3$ in *n*-heptane, where the only observed photoreaction pathway is formation of C. From these experiments, the extinction coefficient for C at 332 nm, the wavelength used to measure quantum yields was determined to be $3.0 \times 10^3 \text{ L mol}^{-1} \text{ cm}^{-1}$.

(5) (a) Eisch, J. J.; King, R. B. *Organometallic Syntheses*; Academic Press: New York, 1965; Vol. 1, p 151. (b) Treichel, P. M.; Shubkin, R. L.; Barnett, K. W.; Reichard, D. *Inorg. Chem.* 1966, 5, 1177-1181.

* Universität Witten/Herdecke.

† University of California.

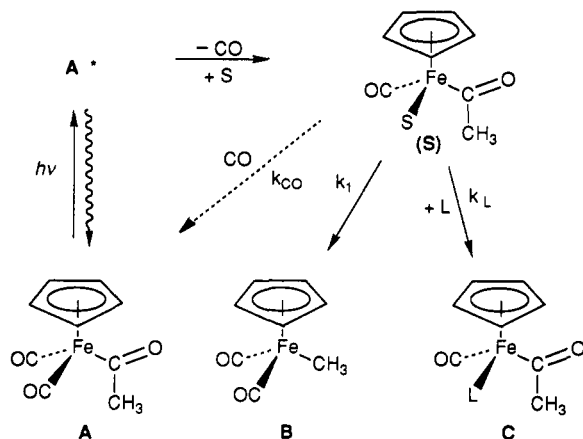
(1) (a) Ford, P. C.; Friedman, A. *Selective Activation of Small Molecules. In Photocatalysis: Fundamentals and Applications*; Serpone, N., Ed.; J. Wiley and Sons: New York, NY, 1989; Chapter 16, pp 541-564.

(2) Henrici-Olivé, G.; Olivé, S. *Catalyzed Hydrogenation of Carbon Monoxide*; Springer-Verlag: Berlin, 1984.

(3) (a) Collman, J. P.; Hegedus, L. S.; Norton, J. R.; Finke, R. G. *Principles and Applications of Organotransition Metal Chemistry*; Univ. Science Books: 1987; Chapter 6; (b) Calderazzo, F. *Angew. Chem., Int. Ed. Engl.* 1977, 16, 299-311. (c) Flood, T. C. *Top. Stereochem.* 1981, 12, 37-118. (d) Flood, T. C.; Jensen, J. E.; Statler, J. A. *J. Am. Chem. Soc.* 1981, 103, 4410.

(4) Belt, S. T.; Ryba, D. W.; Ford, P. C. *J. Am. Chem. Soc.* 1991, 113, 9524-9528.

Scheme I. Model for Reactions of the Intermediate S from the Photolysis of CpFe(CO)₂(COCH₃) According to Ref 4^a



^a In 295 K cyclohexane solution, $k_1 = 5.6 \times 10^4 \text{ s}^{-1}$, $k_{\text{CO}} < 6 \times 10^5 \text{ L mol}^{-1} \text{ s}^{-1}$, and $k_2 = 2.4 \times 10^6 \text{ L mol}^{-1} \text{ s}^{-1}$ for $L = \text{PPh}_3$.

Photolyses were carried out in a thermostated (25 °C) high-pressure cell compartment via procedures described previously.⁶ The deaerated CpFe(CO)₂(COCH₃) solutions were irradiated in a pillbox spectrophotometer cell, which permits transmission of pressure changes from the external pressurizing medium to the solution inside, and stirred during irradiation with a Teflon-coated magnetic stirbar. The pillbox cell allows one to prepare a sample without gas bubbles so that pressure-induced concentration changes are solely due to the compressibility of the solution, even when the solution has been equilibrated with an atmosphere of a gas such as CO (see below). A 100-W mercury lamp was used for photolysis, and light at 313 nm was selected by using an Oriel interference filter. Relative quantum yields as a function of pressure were determined by irradiating a fresh solution ($1.5 \times 10^{-4} \text{ M}$) at a specific applied pressure (5–100 MPa) for a series of fixed time intervals and determining the changes in the solution absorbance after each interval. Overall conversion to products was kept to <20%.

Results and Discussion

In the context of the rate constants defined by Scheme I, the quantum yield for formation of B and C can be defined as

$$\Phi_B = \Phi_S \frac{k_1}{(k_1 + k_{\text{CO}}[\text{CO}] + k_L[\text{L}])} \quad (2)$$

$$\Phi_C = \Phi_S \frac{k_L[\text{L}]}{(k_1 + k_{\text{CO}}[\text{CO}] + k_L[\text{L}])} \quad (3)$$

where Φ_S is the quantum yield for the formation of the intermediate S. In the absence of added L, Φ_B is independent of P_{CO} up to 1 atm ($[\text{CO}] \approx 0.01 \text{ M}$) and equals $0.63 \pm 0.03 \text{ mol/einstein}$ in alkane solvents as well as in stronger donors such as acetonitrile and tetrahydrofuran at ambient hydrostatic pressure.⁴ Therefore, $k_1 \gg k_{\text{CO}}[\text{CO}]$, and eq 2 simplifies to

$$\Phi_B = \Phi_S \frac{k_1}{(k_1 + k_{\text{CO}}[\text{CO}])} = \Phi_S \quad (4)$$

The volume of activation for any dynamic process is defined by

$$\Delta V_i^\ddagger = -RT \left(\frac{d \ln k_i}{dP} \right)_T \quad (5)$$

where k_i is the rate constant of interest. The “apparent” volume of activation for quantum yields is calculated from pressure-induced changes according to^{7,8}

$$\Delta V_\Phi^\ddagger = -RT \left(\frac{d \ln \Phi_i}{dP} \right)_T \quad (6)$$

In this context, the effect of hydrostatic pressure on Φ_S was explored by comparing the photolysis-induced absorbance changes in *n*-heptane solutions of A under argon in the high-pressure apparatus at different P from 5 to 150 MPa. Between 5 and 100 MPa, the change in Φ_S with P was a decrease of 5% which would give an apparent ΔV_Φ^\ddagger of $+1.2 \pm 0.5 \text{ cm}^3 \text{ mol}^{-1}$. At pressures above $\sim 100 \text{ MPa}$, Φ_S inexplicably fell off more rapidly with P ($\Delta V_\Phi^\ddagger \approx 4 \text{ cm}^3 \text{ mol}^{-1}$). For this reason, subsequent studies of the competition between the k_1 and k_L pathways were confined to pressures below 100 MPa, in order to avoid possible complications such as discontinuities in solvent properties.

A series of photolysis experiments were carried out using a fixed irradiation time (40 min) at 313 nm to probe the relative absorbance changes at 332 nm (the λ_{max} for A) for a $1.5 \times 10^{-4} \text{ M}$ solution of A in heptane as a function of $[\text{P}(\text{OCH}_3)_3]$ at ambient pressure. For $[\text{P}(\text{OCH}_3)_3] = 0$, the change in optical density was 0.225 (2.0-cm cell), corresponding to a $[\text{A}]$ decrease of $3.1 \times 10^{-5} \text{ M}$ given the extinction coefficient difference $\Delta \epsilon_{\text{AB}} = -3.7 \times 10^3 \text{ L mol}^{-1} \text{ cm}^{-1}$ between A and B at 332 nm. For a series of different $[\text{P}(\text{OCH}_3)_3]$ but otherwise identical conditions, the resulting ΔAbs_{332} decreases with increasing $[\text{P}(\text{OCH}_3)_3]$ to a limiting value 0.120 at $[\text{P}(\text{OCH}_3)_3] > 0.1 \text{ M}$. (Under these conditions, the optical spectra recorded during photolysis displayed a single isosbestic point at 294 nm, and when the photolysis was carried out at higher concentration, the changes in the IR spectra showed only the CpFe(CO)L(COCH₃) product with a single terminal ν_{CO} at 1941 cm^{-1} .) Thus, the ratio $\Delta \epsilon_{\text{AC}}/\Delta \epsilon_{\text{AB}}$ equals 0.53 which gives $\Delta \epsilon_{\text{AC}} = -1.9 \times 10^3 \text{ L mol}^{-1} \text{ cm}^{-1}$ between A and C in heptane. At $[\text{P}(\text{OCH}_3)_3] = 0.009 \text{ M}$, ΔAbs_{332} equals the average of the two limiting values, a condition met when $\Phi_B = \Phi_C$, i.e., when $k_1 = k_L[\text{L}]$ (Scheme I). Thus, given the value of $k_1 = 5.6 \times 10^4 \text{ s}^{-1}$ previously determined,⁴ k_L for $L = \text{P}(\text{OCH}_3)_3$ can be estimated as $6 \times 10^6 \text{ L mol}^{-1} \text{ s}^{-1}$, a value about twice that seen for $L = \text{PPh}_3$ ($2.4 \times 10^6 \text{ L mol}^{-1} \text{ s}^{-1}$).⁴

Although absolute quantum yields are difficult to measure accurately in the high-pressure cell, the more important issue, the ratio of the various photoreaction product quantum yields can be determined from the relative absorbance changes under well-specific conditions. This is shown by the data in Figure 1, which records the changes in relative absorbance as a function of continuous photolysis time for solutions each prepared at $[\text{A}] = 1.5 \times 10^{-4} \text{ M}$. For time intervals corresponding to low overall conversion to products, these plots are linear, but their slopes are dependent on $[\text{L}]$ and on the applied pressure P . When $[\text{P}(\text{OCH}_3)_3] = 0$, experiments carried out at 5

(7) Ford, P. C. In *Inorganic High Pressure Chemistry, Kinetics and Mechanisms*; van Eldik, R., Ed.; Elsevier: Amsterdam, 1986; Chapter 6, pp 295–338.

(8) van Eldik, R.; Asano, T.; le Noble, W. J. *Chem. Rev.* 1989, 89, 549–688.

(6) Wieland, S.; van Eldik, R.; Crane, D. R.; Ford, P. C. *Inorg. Chem.* 1989, 28, 3663–3666.

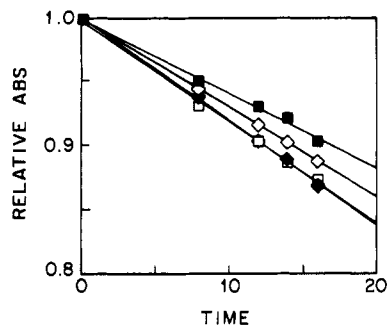


Figure 1. Plots of relative absorbance changes for continuous photolyses of $\text{CpFe}(\text{CO})_2(\text{COCH}_3)$ at 50 and 80 MPa in the presence of $\text{P}(\text{OCH}_3)_3$ (time is in minutes): filled diamonds, $P = 50$ MPa, $[\text{L}] = 0$; open squares, $P = 80$ MPa, $[\text{L}] = 0$; open diamonds, $P = 50$ MPa, $[\text{L}] = 6 \times 10^{-3}$ M; filled squares, $P = 80$ MPa, $[\text{L}] = 6 \times 10^{-3}$ M.

and 80 MPa gave nearly indistinguishable plots, owing to the very low sensitivity of Φ_s to P , but the same is not true for experiments carried out at $[\text{P}(\text{OCH}_3)_3] = 0.006$ M. The slopes of the plots at 5 and 80 MPa both differed from each other and from those carried out without phosphite at the same pressures.

The key information in Figure 1 can be drawn from the slopes of the respective plots

$$\begin{aligned} \text{slope} &= \frac{d(\text{Abs})}{dt} = I_a[\Phi_B \Delta\epsilon_{AB} + \Phi_C \Delta\epsilon_{AC}] \\ &= I_a[(\Phi_B + 0.53 \Phi_C) \Delta\epsilon_{AB}] \end{aligned} \quad (7)$$

given the extinction coefficient information described above. If one defines the ratio of slopes for two experiments at the same P as

$$R^L = \frac{\text{slope}^L}{\text{slope}^0} \quad (8)$$

then for any individual pressure the following relationship can be shown to be valid:

$$R^L = \frac{\Phi_B^L + 0.53 \Phi_C^L}{\Phi_B^0} \quad (9)$$

given the boundary condition that $\Phi_B^0 = \Phi_B^L + \Phi_C^L$ which results from the earlier observation that $k_1 \gg k_{\text{CO}}[\text{CO}]$, where the superscript "L" denotes the experimental result at a particular $[\text{L}]$ and the superscript "0" denotes the experiment for $[\text{L}] = 0$. From the definitions of Φ_B and Φ_C in eqs 2 and 3 plus eq 9, the following relationship can be derived:

$$\frac{k_L[\text{L}]}{k_1} = \frac{R^L - 1}{0.53 - R^L} \quad (10)$$

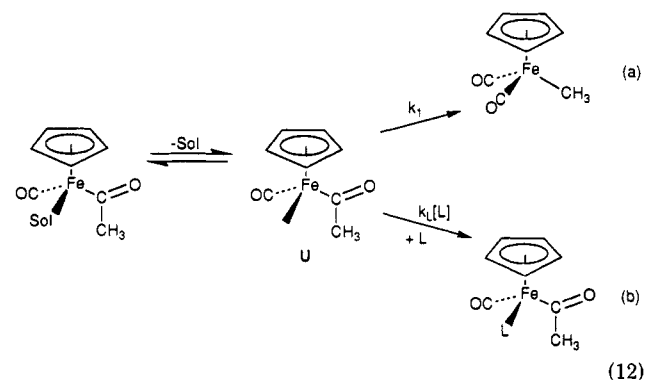
Thus, the quantitative ratios of the rates for the two pathways competing for the intermediate S (Scheme I) can be calculated from the slopes of the plots in Figure 1. At 5 and 80 MPa these ratios are 0.34 and 1.27, respectively, with estimated uncertainties of $\pm 20\%$. Despite these uncertainties, it is quite obvious that pressure has a dramatic ability to tune the partitioning between these two competing reactions, the ratio changing by nearly a factor of 4 over this relatively modest range in hydrostatic

pressure. This can be put into more quantitative terms as follows:

$$\begin{aligned} \Delta V_{\text{rate ratio}}^\ddagger &= -RT \left(\frac{d \ln (k_L[\text{L}]/k_1)}{dP} \right)_T = \\ &= \Delta V_L^\ddagger - \Delta V_1^\ddagger - RT \left(\frac{d \ln [\text{L}]}{dP} \right)_T \end{aligned} \quad (11)$$

where the third term reflects changes in $[\text{L}]$ due to the compressibility of the solvent. Compressibility would be about 10% for heptane over this ΔP , so the third term would have a value about $-3.5 \text{ cm}^3 \text{ mol}^{-1}$. From pressure-induced rate ratio changes determined above, one can calculate a $\Delta V_{\text{rate ratio}}^\ddagger$ value of $-43 \pm 8 \text{ cm}^3 \text{ mol}^{-1}$. This gives a surprisingly large difference in activation volumes for the competitive steps (once the effect of solvent compressibility on $[\text{L}]$ has been subtracted), i.e., $\Delta V_L^\ddagger - \Delta V_1^\ddagger \approx -39 \pm 8 \text{ cm}^3 \text{ mol}^{-1}$.

This dramatic difference between the respective ΔV^\ddagger 's clearly indicates major mechanistic differences for the pathways from S which partition the photoreaction products. Perhaps this is not surprising given the fundamentally different characters of the reactions, ligand substitution of L for coordinate solvent, and migration of a methyl group from the acyl carbon to the metal. In each case a solvent molecule is displaced from the coordination sphere, but the k_1 step generates two species from a single precursor molecule, while ligand substitution requires two precursor molecules to give two product molecules. A significantly positive ΔV_1^\ddagger might well be expected if solvent dissociation to give the unsaturated species U (eq 12) were



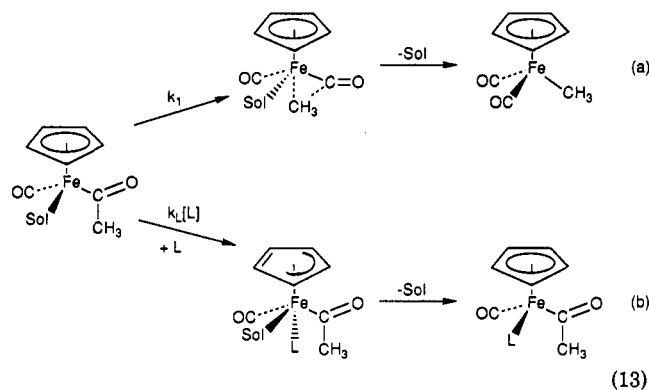
a necessary condition for methyl migration. However, U would also be the intermediate for ligand substitution via a limiting dissociative mechanism; indeed a dissociative or dissociative interchange mechanism has been proposed as the explanation for positive ΔV^\ddagger 's for the substitution of Sol in $\text{Cr}(\text{CO})_5(\text{Sol})$ (Sol = benzene or substituted benzene) generated via flash photolysis of $\text{Cr}(\text{CO})_6$ in a solvent Sol.^{9,10} If both processes were occurring via U as another common intermediate, one would need to explain the large difference in the ΔV^\ddagger 's not according to the nature of U itself, but according to the respective pressure dependences of the steps (12a and 12b) which then partition U. Certainly the bimolecular associative step 12b would be expected to display a much more negative ΔV^\ddagger than the unimolecular rearrangement eq 12a.⁹ However, it seems unlikely that a truly unsaturated species

(9) Zhang, S.; Dobson, G. R.; Zang, V.; Bajaj, H. C.; van Eldik, R. *Inorg. Chem.* 1990, 29, 3477-3482.

(10) Zhang, S.; Zang, V.; Bajaj, H. C.; Dobson, G. R.; van Eldik, R. *J. Organomet. Chem.* 1990, 397, 279.

such as U would display as much selectivity as that demonstrated by S, which is at least 1 order of magnitude more reactive with $\text{P}(\text{OCH}_3)_3$ than it is with CO.¹¹

An alternative would be for the two reactions from S to proceed by markedly different mechanisms, for example, methyl migration by a concerted pathway having a substantially dissociative character (e.g., eq 13a), phosphite substitution via an associative mechanism, possibly via a "ring-slipped" η^3 -coordinated C_5H_5 species (e.g., eq 13b),¹² as has been proposed in photosubstitution mechanisms of the methyl analog B.¹³



The activation volume for the former would be expected to be no less than zero, but more likely to be at least modestly positive since a solvent molecule is being released

(11) (a) Studies by Simon and co-workers^{11b,c} indicate that the unsaturated $\text{Cr}(\text{CO})_5$ intermediate formed in the picosecond flash photolysis of $\text{Cr}(\text{CO})_6$ reacts with very little selectivity to coordinate whichever nucleophile is present, including both the alkane (C-H bonds) and hydroxyl (oxygen lone pairs) fragments of alkyl alcohols. Thus, we would expect relatively little selectivity of a fully unsaturated intermediates such as U. (b) Xie, X.; Simon, J. *J. Am. Chem. Soc.* **1990**, *112*, 1130-1136. (c) O'Driscoll, E.; Simon, J. *J. Am. Chem. Soc.* **1990**, *112*, 6580-6584.

(12) Basolo, F. *Polyhedron* **1990**, *9*, 1503-1535.

(13) Fettes, D. J.; Narayanaswamy, R.; Rest, A. *J. Chem. Soc., Dalton Trans.* **1981**, 2311-2316.

in this step. A distant analogy might be drawn to the ring-closure reaction of the complex $\text{cis-W}(\text{CO})_4(\text{chlorobenzene})(\text{Ph}_2\text{P}(\text{CH}_2)_n\text{CH}=\text{CH}_2)$ where ΔV^\ddagger values of +7.7 and $5.1 \text{ cm}^3 \text{ mol}^{-1}$ were determined for $n = 1$ and 2 , respectively.¹⁴ An analogy to eq 13b would be the reaction of phosphine substitution for CO on $(\eta^5\text{-C}_5\text{H}_5)\text{Rh}(\text{CO})_2$ which has been generally accepted to involve a η^5 to η^3 ring-slip mechanism allowing associative attack of the incoming ligand on the metal center. Pressure effects on this reaction demonstrated negative ΔV^\ddagger values of -14.3 and $-17.0 \text{ cm}^3 \text{ mol}^{-1}$ for PPh_3 and PBU_3 , respectively.¹⁵ Thus, a scheme such as described by eq 13 would be consistent with a large $\Delta V^\ddagger_{\text{L}} - \Delta V^\ddagger_{\text{1}}$ difference in activation volumes for the competitive steps, although the $-39 \pm 8 \text{ cm}^3 \text{ mol}^{-1}$ value still seems remarkable.

In summary, the pressure data points to markedly different mechanisms for the two reactions partitioning the intermediate S, the methyl migration having a dissociative character and the phosphite substitution pathway proceeding by a more associative mechanism. Whether this type of difference is reflective of behavior characteristic of only the $\text{CpFe}(\text{CO})_2(\text{COCH}_3)$ system, for which a ring-slippage mechanism is possible, or carries over to analogous intermediates of other metal acyl complexes will need to be tested for a system such as $\text{Mn}(\text{CO})_5(\text{COCH}_3)$.¹⁶

Acknowledgment. This research was sponsored by a grants to R.v.E. and P.C.F. from NATO, to P.C.F. (DE-FG03-85ER13317) from the Division of Chemical Sciences, Office of Basic Energy Sciences, U.S. Department of Energy, and to R.v.E. from the Deutsche Forschungsgemeinschaft and the Volkswagen-Stiftung. We thank Karen McFarlane for carrying out some important experimental controls.

OM920371R

(14) Zang, V.; Zhang, S.; Dobson, C. B.; Dobson, G. R.; van Eldik, R. *Organometallics*, **1992**, *11*, 1154-1158.

(15) Vest, P.; Anhaus, J.; Bajaj, H. C.; van Eldik, R. *Organometallics* **1992**, *10*, 818-819.

(16) Lee, B. Studies in progress.